A combined Monte Carlo/DFT approach to simulate UV-vis spectra of molecules and aggregates: merocyanine dyes as a case study

Bernardino Tirri, Gloria Mazzone, Alistar Ottochian, Jerôme Gomar, Umberto Raucci, Carlo Adamo, Ilaria Ciofini

A combined Monte Carlo/DFT approach to simulate UV-vis spectra of molecules and aggregates: merocyanine dyes as a case study.

Bernardino Tirri[a], Gloria Mazzone[a], Alistar Ottochian[a], Jerôme Gomar[b], Umberto Raucci[a,*], Carlo Adamo[a,c], Ilaria Ciofini[a,*]

a) *Chimie ParisTech, PSL University, CNRS, Institute of Chemistry for Life and Health Sciences, Theoretical Chemistry and Modelling, 75005 Paris, France;*
b) *L'Oréal, Research and Innovation, 1 Avenue Eugène Schueller, 93601 Aulnay-sous-Bois, France*;
c) *Institut Universitaire de France, 103 Boulevard Saint Michel, F-75005 Paris, France.*

Abstract

The combination of a Monte Carlo (MC) sampling of the configurational space with Time dependent Density Functional Theory (TD-DFT) to estimate vertical excitations energies has been applied to compute the absorption spectra of a family of merocyanine dyes in both their monomeric and dimeric forms. These results have been compared to those obtained using a static DFT/TD-DFT approach as well as to the available experimental spectra.

Though suffering of the limitations related to the use of DFT and TD-DFT for this type of systems, our data clearly show that the classical MC sampling provides a suitable alternative to classical molecular dynamics to explore the structural flexibility of these donor-acceptor (D-π-A) chromophores enabling a realistic description of the Potential Energy Surface of both their monomers and aggregates (here dimers) and thus of their spectra.

Overall, the combination of MC sampling with quantum mechanics (TD-DFT) calculations, carried out in implicit dioxane solvent on random snapshots, provides a workable compromise to solve the combined challenge of accuracy and time-consuming problem not only for merocyanines momers but also for their dimers, up to now less investigated. Indeed, the simulated absorption spectra fairly agree with the experimental ones, suggesting the general reliability of the method.

Corresponding authors: umberto.raucci@unina.it ; ilaria.ciofini@chimieparistech.psl.eu

1. Introduction

Merocyanines are a class of polar dyes showing a variety of colors, with exceptional non linear optical responses, photo-dimerization, photo-isomerization, solvatochromism, and thermochromism properties, and unique self-assembly behavior arising from their large dipolar character, leading to have been employed extensively as spectral sensitizers for silver halide photography, as hybrid large band gap semi-conductor materials, in optical disks as recording media, in industrial paints, for trapping of solar energy, as laser materials, as photorefractive materials, as antitumor agents, as probes for biological systems, as sun filters.[1] This class of molecules is characterized by the presence of a donor and an acceptor group connected by an ethylene or polyethylene bridge (see Figure 1 for a schematic representation of these molecules). Thus, the so-called Bond-Length Alternation (BLA), accounting for the difference between single and double carbon-carbon bonds of the polyethylene bridge, represent a relevant structural parameter of merocyanines. Small (large) BLAs are an indication of an increased (reduced) delocalization of the π electrons and of an improved (worsen) coupling between the donor-acceptor moieties, thus leading to a red (blue) shift of the spectra. In terms of the electronic structure, a small BLA indicates a formally neutral structure, while a large BLA suggests an increasing weight of the charge-separation (zwitterionic) form.[2] Nonetheless, BLA is by itself a challenging property for computational approaches such as Density Functional Theory (DFT), since its correct reproduction requires the reduction (or even cancellation) of the Self-Interaction Error (SIE), which, inducing a large electronic delocalization, leads to shorter BLAs.[3,4]

In the last decade, several efforts have been devoted to the theoretical description of the merocyanine family of dyes using DFT and TD-DFT, a class of numerical methods that allows for a reliable prediction of electronic absorption spectra not only in term of band position (i.e. λ_{max}) but also in intensity and band shape in simple and complex media.[5-7] Several studies focus on the definition of the most suitable exchange-correlation functional for modelling the merocyanines electronic absorption spectra. Since the most intense transition in merocyanines is expected to show a CT character standard DFT approaches are expected to fail.[8] However, previous studies have shown that functionals normally curing (or mitigating) CT problems, including range separated hybrids and optimally-tuned functionals, do not significantly improve the results for merocyanines.[5,9,10] Actually, it has even been suggested that the insensibility of the computed transitions to the choice of the DFT approach is a fingerprint of the merocyanine.[11]

Furthermore, the fine-structure of their absorption spectra is still matter of debate. Indeed, while from one side, theoretical model studies and fine analysis of experiment outcomes suggest that the broadening of the first absorption band is mainly related to the C=C vibration of the polymethine chain[11-12], from another side, studies using complete modelling of the band shape of the absorption spectrum using a Franck-Condon (FC) approach indicate that the origin of this structured band can be ascribed to a number of different vibrational modes.[10,13-16] In some cases, difficulties have been evidenced, so that approximate FC models are used. For instance, vibrational levels are considered as being equal for both the ground and excited states (adiabatic approximation) or only one degree of freedom is explicitly considered.[15,16] As rule of thumb, the vibronic coupling is expected to shift the λ_{max} of about 0.3 eV.[15]

Furthermore, simulating the merocyanines behavior in complex media is even more complicated considering that: i) merocyanines undergo to strong solvatochromism[17], and the solvent effects cannot be in turn avoided in the modelling;[16,18-19] ii) in solution merocyanines form H- and J-type aggregates (dimers), differing in the relative orientation of the dipole moment of the two constituting monomers (antiparallel for H-aggregates, parallel for the J-type)[20-21]. All these issues are strongly entwined and, often, they have been investigated separately.

Here, focusing on both the monomeric and dimeric forms of the merocyanines **1**-**4** reported in Figure 1, we tried to disentangle the intricate relationships between the structural and electronic features of merocyanines exploring their complex phase space with a stochastic approach relying on Monte Carlo (MC) molecular simulations. The flexible structure of merocyanines adds another level of complexity in the modeling. Indeed, standard methods to obtain the vibrationally resolved optical spectra[22-25] cannot be applied in this situation due to the presence of several energetically accessible minima existing on the ground and/or excited state potential energy surfaces (PESs).[26-28] In such cases a single structure can hardly be representative of the real phase space and ensemble averages become mandatory. For this reason, we simulated the absorption spectrum as an average of those vertically computed for a statistically representative average over an ensemble of molecular structures, extracted from the ground state PES. In this respect, the widely applied strategy to build the statistical ensemble is based on Molecular Dynamics (MD) simulations, where the time evolution of the system is achieved by integrating the classical Newton's equations of motion, the corresponding potential energy being computed either at classical or quantum chemistry level of theory.[26-30] Although MD simulations are widely and successfully applied, some concerns still arise. Indeed, when large energy barriers (often of several k_BT) to conformational changes (e.g. bond rotations in flexible molecules,

geometrical rearrangements in aggregates) exist, it is easy to be trapped in local -low energy- conformations, leading to a poor quality statistical sampling. Increasing the temperature of the simulation, in conjunction or not with simulated annealing approaches or replicate trajectories starting from different initial conditions are common procedures to improve the space-phase sampling.[31] Driven dynamics (metadynamics, umbrella sampling) are also viable alternatives, requiring the identification of the relevant reaction coordinate(s).[32,33] Nevertheless, spectra simulated at high temperature are clearly broadened with respect to the experimental ones, and more replicas of the trajectory or driven dynamics can be computationally difficult to achieve especially in the case of ab initio molecular dynamics.

For these reasons, we relied on an alternative philosophy to escape from local minima on the PES based on random sampling with the Monte Carlo method. In this approach, configurations in the phase space are generated by randomly changing the coordinates of a randomly chosen atom of the system, and accepting the new configuration according to the Metropolis sampling algorithm.[34] The random moves and the possibility to accept higher energy configurations allow MC simulations to avoid being trapped on local minima reaching energetically distinct regions of the PES, which allows the simulation of the photo-physical properties of complex chromophores in realistic environments such as condensed phases (solution, crystal or amorphous phases), or in matrix (biological or polymeric).

Although this approach is very powerful, few examples are reported in literature coupling MC sampling with quantum chemistry calculation for the simulation of UV-Vis absorption spectra of molecules, mainly focused on the organization of the solvent molecules around the chromophore.[35-37]

The main aim of the present work is thus to show the potentiality of a combined Monte Carlo/Quantum Chemistry, here Time Dependent Density Functional Theory (TD-DFT), approach to simulate the electronic absorption spectra of the merocyanines family of flexible molecules and their aggregates (here dimers).

2. Computational details

Two computational protocols were considered for the calculation of UV-Vis spectra. The first one, referred to as *static*, consists of a full optimization of the molecular structures using the PBE0 functional[38] and the 6-31+G(d,p) basis set.[39] In the case of dimers, dispersive interactions were accounted through the original Grimme empirical correction (GD3).[40] Vertical absorptions were then computed at the TD-DFT level, using global (PBE0) and range separated (ωB97XD)[41] hybrid functionals in conjunction with the 6-31+G(d,p) basis set. The first

functional, PBE0, is widely used for the computation of UV-Vis spectra involving valence transitions,[42] while the second, containing a larger quantity of HF exchange, is more suitable for Charge Transfer (CT) excitations and it was already applied to study model merocyanines.[5] Solvent effects were taken into account using the IEF-PCM model, considering dioxane as solvent as in the experimental protocol.[47] Due to the aprotic nature of this solvent, no specific solute-solvent interactions are expected, so that the IEF-PCM provides accurate results for the electronic transitions.[43]

The second approach, hereafter referred to as *stochastic*, is based on the generation of ensemble configurations for both monomer and dimeric forms of merocyanines **1-4** (Figure 1) using MC Metropolis simulations. Our method is schematized in Figure 2 and works as it follows: i) the statistical ensemble is built through the MC sampling of the ground state PES, ii) vertical excitations on randomly selected configurations are carried out at quantum mechanics level, iii) the electronic absorption spectrum is obtained convoluting by a gaussian broadening the so computed vertical excitations.

The energy of the MC configurations, was computed at molecular mechanics level using standard Generalized Amber Force Field (GAFF).[44] Production MC simulations were carried out for $1*10^7$ steps at a 300 K temperature. Then, 500 structures were randomly extracted to simulate the UV-Vis spectrum and their vertical electronic transitions were computed using the same TD-DFT computational level as for the *static* approach, including solvent effects. Convergence of the sampling was tested for the monomer 1 molecule by using a sampling of 600 providing the same computed spectral properties.

Finally, the resulting absorption spectrum (A(E)) was simulated as:

$$A(E) = \frac{1}{\mathrm{N_p}} \sum_{k}^{\mathrm{N_P}} \left[\sum_{\mathrm{L \neq I}}^{\mathrm{N_S}} f_{\mathrm{IL}}(\boldsymbol{R_k}) g(E - \Delta E_{\mathrm{IL}}(\boldsymbol{R_k}), \boldsymbol{\delta}) \right]$$

where vertical excitation energies ($\Delta E_{\mathrm{IL}}(\mathbf{R}_k)$) between the ground electronic state (I) and excited state (L) and corresponding oscillator strengths ($f_{\mathrm{IL}}(\mathbf{R}_k)$) were computed for each sampled configuration ($\mathbf{R}_k$), N_s is the number of excited states considered, N_P is the number of sampled points, and g represents a normalized gaussian function centered on ΔE_{IL} of full width at half maximum (δ) of 0.3 eV.

All DFT and TD-DFT calculations were carried out using the Gaussian program,[45] while MC computations were performed using the LAMMPS code.[46]

3. Results and Discussion

3.1 UV-Visible spectra: static vs stochastic approach.

In Table 1 are collected the computed absorption energies maxima (λ_{max}) for monomers and dimers of the merocyanines sketched in Figure 1, obtained with the two approaches described above (*static* and *stochastic*).

From literature data it's known that merocyanine dyes undergo vibronic coupling significantly affecting the position of the λ_{max} computed by a static approach . The red-shift of the main peak, with respect to the vertical approximation, was estimated to be about 0.3 eV.[15] The comparison of data coming from *static* calculations with the experimental wavelengths,[47] included in Table 1, not surprisingly reveals that the vertical transitions energies computed at the PBE0 level for all the monomers are significantly overestimated (between 0.42 and 0.50 eV). The computed Mean Absolute Deviations (MADs) are quite large, but essentially in agreement with the errors reported in the literature for similar systems.[5,9,10] Furthermore, if the estimated 0-0 correction is subtracted (0.3 eV), the deviations are within the expected range of accuracy for TD-DFT methods (0.1-0.2 eV), always taking into account the above reported caveats. These discrepancies slightly increase if the range-separated ωB97XD functional is considered (+0.47 eV for **1**), in agreement with data in literature.[5] For these reasons, ωB97XD will be not further considered for the other molecules and only PBE0 results will be discussed.

Despite these significant deviations between theory and experiments, the experimental relative trends are correctly reproduced by the PBE0 results. Indeed, the outcomes obtained (Table1) show significant blue-shifts going from molecule **1** to **4** (between 0.09 and 0.56 eV), in the same range of the experimental observation obtained by Wortmann and co-workers (between 0.01 and 0.56 eV),[47] with the exception of molecule **2**, for which a red-shift of 0.22 eV is found, in agreement with the experimental trend.

The topology of the Frontier Molecular Orbitals (FMOs) of the investigated molecules is depicted in Figure 3. According to the TD-DFT calculations, the most intense absorption corresponds to a $\pi \rightarrow \pi^*$ transition, from the highest occupied molecular orbital (HOMO) to the lowest unoccupied molecular orbital (LUMO). These FMOs are delocalized over the whole core of the molecules, including the polymethine unit and the pyridinic residues (or the amino group for molecules **3**). Therefore, any structural deformation modifying the electronic conjugation of the backbone impacts the computed absorption λ_{max}. On the other hand the CT character appears limited.

The trend found for monomers are kept for the dimers. All the static calculations reported in Table 1 refer to co-facial antiparallel dimers (H-aggregate, see next paragraph for further explanation on structures), representing the global minimum on the ground state PES. A significant overestimation of the λ_{max} is found at the PBE0 level, even if the deviations, falling within 0.32 eV (**1** and **2**) and 0.45 eV (**3b**), are slightly smaller than the corresponding monomers. Indeed, the final MAD for dimeric species is 0.38 eV, to be compared with 0.46 eV for the monomeric ones. As experimentally observed, all vertical transitions are blue-shifted in going from the monomer to the dimer, although this variation is slightly overestimated with respect to experiments.[47] Comparing the dimers absorption spectra, the one of dimer **2** is characterized by a red-shift (0.30 eV) of the maximum absorption, with respect to **1**, the same found in the experiments.[47] In contrast, the molecule **3b** is slightly blue shifted at theoretical level (0.03 eV), while it results red-shifted (0.10 eV) with respect to the recorded spectrum.[47]
Resuming, static TD-DFT calculations on the monomeric and H-type dimeric forms of merocyanines provide a picture in qualitative agreement with the experimental data, even if the obtained errors are quite large, though in line with previous literature data.
A sizable improvement, compared to the *static* approach, is obtained simulating the electronic absorption spectra as an ensemble average over multiple configurations. As matter of fact, the MAD is halved going from the *static* to the *stochastic* approach for both monomers and dimers. In details, the MAD is 0.46 eV for the static monomers whereas it becomes 0.26 eV using a MC sampling. For a neat comparison the vertical transitions are computed at the same PBE0/6-31+G(d,p) level of theory in both the *static* and the MC spectra. As in the case of the *static* approach, the largest error (+0.3 eV) is obtained for the compound **3b**, suggesting the subtle effects played by the length of the polymethine bridge and the BLA. The relative shifts computed for the different merocyanines in their monomeric forms also fairly agree with the *static* approach and the experimental results. The character of the brightest electronic transition corresponds to a $\pi \rightarrow \pi^*$ transition, where HOMO and LUMO orbitals are delocalized over the whole core of the molecule (FMOs of a representative geometry are reported in Supporting Information see Figure SI.1 and SI.2).
The MC sampling leads to even better results in the case of dimers, for which the MAD decreases from 0.38 eV (*static* approach) to 0.17 eV (*stochastic* approach). In this case, the capability of MC to account for several configurations accessible is crucial to reduce the simulated/experimental error on λ_{max}. Compound **3b** represents the trickiest molecule to simulate (error of +0.22 eV), also in its dimeric form. Overall the MC results are in fairly

agreement with the experimental spectra both in terms of absolute computed-experimental shifts than in relative shifts between the different merocyanines.

3.2 Structural effects underpinning spectra

After the discussion of the *static* and *stochastic* TD-DFT results on the band position, it is interesting to examine how the structural features of merocyanines and their dimeric species influence the λ_{max} and how the two different approaches are able to describe them. As above-stated, the major limitation of the *static* approach essentially relies on the impossibility to consider all the energetically accessible minima existing on both ground and/or excited PESs. The MC simulations, though cannot be able to provide the ZPE corrections due to their quantum nature, allows overcoming such a limitation taking into account several energetically accessible conformations, thus supplying the contribution to λ_{max} coming from the distortions of flexible geometrical parameters.

As matter of facts, several degrees of freedom can drastically influence the electronic properties of this family of chromophores. Relevant parameters, to be taken into consideration, are: i) the bond length alternation (Figure 4a), ii) the relative orientation between the pyridone and the pyridine rings (amino group for **3**), linked by the conjugated chain (defined by the angle θ, Figure 4b) and iii) for the dimer, the relative distance (and orientation) of the two monomers. Small (large) BLAs are indication of increased (reduced) delocalization of the π electrons and of an improved (worsen) coupling between the two moieties, thus leading to a red (blue) shift of the spectra. A similar effect on the electronic structure could be expected by a coplanar rearrangement of the pyridone and the pyridine rings (or amino moiety for **3**), where smaller θ values correspond to smaller transition energies. Short intermolecular distances, represented as the distance between the centre of mass (CoM) of the two monomers, lead to low energy transitions while an opposite effect is expected for larger inter-dimer distances.

The main geometrical parameters computed for merocyanines **1**-**4** are collected in Table 2 whereas the structures of the monomers are depicted in Figure 4. In the case of MC simulations average values are reported (see Supporting Information Figure SI.2 for their representation). Going from static to MC calculations, small variations of the angle θ are observed, the largest ones being of about ± 4 degrees (for **2**, **3a** and **3b**), thus suggesting that this parameter, at least for monomers, is not relevant.

Concerning BLAs, the small lengths of the polymethine chain should prevent large errors at DFT level, generally observed in longer oligomeric chains[48,49] and, indeed, PBE0 and ωB97XD

functionals give very close values for molecule **1**, even if their errors become significantly different when larger systems are considered. Larger variations are, instead, observed in going from static to MC calculations, with different behavior for the considered systems. In particular, the BLAs increase for **2**, **3b** and **4** and decrease for **1** and **3a**, although in some cases the variations are quite small. Overall, a small energy difference (about 3 kcal/mol) between the PBE0 optimized and the MC average structures is found for all the molecules. This energy difference is not only related to the BLA since the two structures differ also in other geometrical parameters (i.e., lateral chains conformation), as can be inferred from the structures reported in Figure 4c-f. More interestingly, it cannot be traced from our results a direct relationship between any single selected structural parameter, including the BLAs or θ angles, and the red-shifts observed in going from static to MC values. Such a shift results from a global deformation rather than a single dominant degree of freedom. In other words, the hypothesis of a dominant effect of the C=C double bond variation on the merocyanine spectra cannot be confirmed by our calculations. Furthermore, it should be recalled that structures obtained via the stochastic approach are produced at classical molecular mechanics level thus the observed effect on the spectra is the sum of small structural effect due to the difference between the full DFT and the MM based MC approach and the dominant effect related to the need of a more exhaustive sampling allowed by the MC approach. Of course favorable error cancellation in this procedure cannot be excluded.

Therefore, the net effect of stochastic calculations is the red-shift of the λ_{max} providing better agreement with the experimental spectra. It should be also pointed out that the resulting MAD is of the same order of magnitude as the E^{0-0} estimated for similar systems (0.3 eV).[15]

In an attempt to provide a comparison even with the vibrationally resolved absorption spectrum, the structure of the lowest electronic excited state (S_1) of molecule **1** was optimized at the PBE0/6-31G level (see Supporting Information Figure SI.1 for their representation). However, because of the flexibility of the molecule, the obtained S_1 minimum energy structure is strongly distorted with respect to the ground state one (θ close to 90°). As a consequence, the FC approximation is no longer valid and it is not possible, at least with usual approaches, to compute the vibronic contribution.

Once defined the global molecular flexibility as the main factor affecting the absorption energies of the merocyanine monomers, it is interesting to establish how these structural features can impact the aggregate formation.

All the molecules considered are push-pull systems possessing a very high dipole moment on the ground electronic state (20.3 Debye for **1**). Previous studies have shown that dipole-dipole interactions are indeed the driving force for their self-assembly in dilute solution leading to dimers showing an antiparallel orientation of the dipole moment of the constituting monomers and thus an overall null dipole moment. Furthermore, the presence of a null dipole moment of dimers avoids their further clustering and thus the formation of larger aggregates.[21]

In agreement with the experimental observation, the MC sampling on the merocyanine dimers indicates that most of the stable dimeric forms are cofacial and antiparallel aligned (H aggregates) while only a few of them have a parallel arrangement of the two units (J dimer). In particular static calculations, performed at PBE0/6-61++G(2d,2p) level of theory, indicate that the H aggregates are most stable than the J ones of 18.1 kcal/mol and this is confirmed by the MC calculations showing less than 1% of parallel dimers. Furthermore, due to the relative high difference in energy between the two forms it is clear that it is difficult to go from one to the other arrangement.

Due to the statistical sampling which massively favor the H dimers, in agreement with the experimentally observed blue-shift, only these latter will be considered in the following. These dimers appear even more flexible than the isolated monomers, since they undergo large structural modifications, as illustrated by the data reported in Table 2 and Figure 5. Indeed, significant variations are observed for both θ and BLAs. Starting from the first parameter, the static structures of dimers **2**, **3a** and **3b** are characterized by large torsional angles (θ around 50 degrees), while dimers **1** and **4** still retain an almost planar arrangement of their moieties (θ around 10 degrees). As above-mentioned, their corresponding isolated monomers are all almost planar. The weak non-covalent interactions between the pyridine rings force the planar structure of the monomers in molecules **1** and **4**, while the flexible amino terminal chain in dimers **3** prevents such arrangement. In molecule **2**, instead, the head-tail rearrangement is characterized by a steric repulsion between the ethyl and butyl chains substituting group of the two aromatic rings, which induces a shearing of the two moieties. As a consequence, the leucoline moieties can rotate around a C-C bond of the polymethine chain. These distorted structures break the extended π conjugation and induce a significant increase of the BLAs in the dimers exhibiting the largest values of θ (for molecules **1**, **2**, **4**). Therefore, the zwitterionic form is favored over the neutral one.

The intermolecular distance was computed as the distance between the centers of mass (CoM) of the two moieties. Shorter distances correspond to a more compact structure, whereas the

longer distances arise from a relative shift of the two units to reduce the steric hindrance. Thus, the intermolecular distance strongly depends on the steric repulsion in the packed structures, so that a large panel of values is found, ranging from 3.9 (molecule **3b**, the most compact) to 5.6 Å (molecule **2**). It is interesting to note that the MC structures are relatively higher in energy compared to the optimized ones. The difference in total energies between the two sets is just twice than the value observed for the monomer (7-9 kcal/mol, see Table 2), the exception being the dimer **2** where very compact rearrangement (CoM = 4.3 Å) lead to significantly higher energies (ΔE = 14.2 kcal/mol).

Going from the monomers to the dimers, all the transitions are blue-shifted, so it seems that the mutual polarization of the two monomers in the aggregate plays the major role. Therefore, we have simulated the electronic spectra of the monomer at the geometry in the corresponding dimer, for both optimized static and MC structures. As it appears from the results collected in Table 2, all the transitions are close (within a few thousandths of eV) to those computed for the corresponding isolated monomers, regardless of the approach used to obtain such a structure (static or MC). As for the isolated monomer, it is not possible to draw a direct relationship between the BLA and the θ parameters, the main factor affecting the blue-shifts of the dimers seems to be their formation, accounted by the distance of the CoMs. Nevertheless, there is not a correlation between the blue-shifts in the transitions and the energy of formation of the dimers. Similarly, no correlations were found between the static and MC transitions for the dimers and their corresponding CoMs distances (or their differences). However, the numerical improvement in computed absorption energies appears evident looking at the computed MAD (0.17 eV for the MC dimers), well below the expected value for such systems. Figure 6, where the computed spectra for the dimer **1** are reported, also exemplifies this improved agreement

4. Conclusions

In conclusion, the overall agreement between MC results and experimental data suggests that the main structural effects on the electronic spectra are captured by the MC approach combined with vertical TD-DFT calculations. Although classical MC simulations do not allow to reconstruct the vibronic progression, they take into account the flexible nature of the molecules and its effect on the λ_{max} which is overall shifted leading to a better agreement with the experimental spectra. Our results reveal that despite its simplicity a combined MC/TD-DFT approach is reliable to describe flexible systems that cannot be properly described in a FC static framework. Indeed, in the case of the merocyanines dyes the characterization of the FC

minimum leads to an error bar (0.3-0.5 eV) for the spectra of the monomers obtained with standard functionals, including global or range-separated hybrids, in perfect agreement with literature data.[22,50]

Finally, to the best of our knowledge, a detailed FC analysis of merocyanines dimers has never been performed, the only study concerning two units bound by aliphatic chains which significantly damp intermolecular soft modes. This is not surprising, in view of the difficulties that can be expected in the optimization of the dimers on the excited electronic states. In this respect, the MC stochastic sampling here proposed is a reliable alternative to sample the dimer conformational space. Promising applications can be expected in the future, where the MC approach could be used to generate initial conditions for ab initio molecular dynamics.

Acknowledgements

I.C. gratefully acknowledge support from the European Research Council (ERC) for funding under the European Union's Horizon 2020 research and innovation programme (grant agreement No 648558, STRIGES CoG grant).

Data availability statement. The authors confirm that the data supporting the findings of this study are available within the article and its supplementary materials. Raw data are available from the corresponding author, upon request.

References.

1) Mishra, A.; Behera, R.K.; Behera, P. K.; Mishra, B. K.; Behera, G.B. Chem. Rev. **2000**, 100, 1973.

2) Brückner, C. ; Engels, B. *J. Phys. Chem. A* **2015**, *119*, 12876.

3) Ciofini, I.; Adamo, C.; Chermette, H. *J. Chem. Phys.* **2005**, *123*, 121102.

4) Jacquemin, D. ; Perpète, E.A. ; Ciofini, I. ; Adamo, C. *Chem. Phys. Lett*. **2005**, *405*, 376.

5) Adamo, C.; Jacquemin, D. *Chem. Soc. Rev*. **2013**, *42*, 845.

6) Barone, V. *Wiley Interdiscip Rev.: Comput Mol Sci.* **2016**, *6*, 86.

7) Bloino, J.; Baiardi, A.; Biczysko, M. *Int. J. Quantum Chem.* **2016**, *116*, 1543.

8) Autschbach, J. *ChemPhysChem* **2009**, *10*, 1757-1760

9) Moore II, B.; Autschbach, J. *J. Chem. Theory Comput.* **2013**, *11*, 4991.

10) Le Guennic, B. ; Jacquemin, D. *Acc. Chem. Res*. **2015**, *48*, 530.

11) Mustroph, H.; Reiner, K.; Senns, B.; Mistol, J.; Ernst, S.; Keil, D.; Hennig, L. *Chem. Eur. J.* **2012**, *18*, 8140.

12) Mustroph, H.; Towns, A. *ChemPhysChem* **2018**, *19*, 1016.

13) Ishchenko, A. A.; Kulinich, A. V.; Bondarev, S. L., Raichenok, T. F. *Spectrochim. Acta A: Mol. Biomol. Spectr*. **2018**, *190*, 332.

14) Capobianco, A.; Borrelli, R.; Landi, A.; Velardo, A.; Peluso, A. *J. Phys. Chem. A* **2016**, *120*, 5581−5589.

15) Champagne, B. ; Guillaume, M. ; Zutterman, F. *Chem. Phys. Lett*. **2006**, *425*, 105.

16) Masunov, A.E.; Anderson, D. Freidzon, A. Ya.; Bagaturyants, A. A. *J. Phys. Chem. A* **2015**, *119*, 6807.

17) Kulinich, A. V.; Kurdyukov, V. V.; Ishchenko, A. A. *New J. Chem*. **2019,** *43*, 7379.

18) Wada, T.; Nakano, H.; Sato, H. *J. Chem. Theory Comput.* **2014**, *10*, 4535.

19) Tanaka, Y.; Kawashima, Y. ; Yoshida, N. ; Nakano, H. *J. Comp. Chem.* **2017**, *38*, 2411.

20) Rösch, U. ; Yao, S. ; Wortmann, R ; Würthner, F. *Angew. Chem. Int. Ed.* **2006**, *45*, 7026 – 7030

21) Würthner, F. *Acc. Chem. Res.* **2016**, *49*, 868.

22) Santoro, F. ; Lami, A. ; Improta, R.; Bloino, J.; Barone, V. *J. Chem. Phys.* **2008**, *128*, 224311.

23) Peltier, C. ; Lainé, P.P. ; Scalmani, G. ; Frisch, M.J.; Adamo, C.; Ciofini, I. *J. Mol. Struc. :Theochem*, **2009**, *914*, 94.

24) Di Tommaso, S. ; Bousquet, D.; Moulin, D.; Baltenneck, F.; Riva, P.; David, H.; Fadli, A.; Gomar, J.; Ciofini, I.; Adamo, C. *J. Comp. Chem*. **2017**, *38*, 998.

25) Baiardi, A. ; Bloino, J.; Barone. V. *J. Chem. Theory Comput*. **2013**, *9*, 4097.

26) Cerezo, J. ; Avila Ferrer, F. J.; Prampolini, G.; Santoro, F. *J. Chem. Theory Comput*. **2015**, *11*, 5810.

27) N. De Mitri, S. Monti, G. Prampolini, V. Barone, *J. Chem. Theory Comput*. **2013**, *9*, 4507.

28) M. Cascella, M.A. Cuendet, I. Tavernelli, U. Rothlisberger J. Phys. Chem. B **2007**, *111*, 10248.

29) Chiariello, M.G. ; Rega, N. *J. Phys. Chem. A* **2018**, *122*, 2884.

30) Chiariello, M.G.; Raucci, U. ; Coppola, F. ; Rega, N. *Phys. Chem. Chem. Phys*. **2019**, *21*, 3606-3614

31) Haverkort, F. ; Stradomska, A. ; de Vries, A. H.; Knoester, J. *J. Phys. Chem. B* **2013** *117*, 5857.

32) Branduardi, D. ; Bussi, G.; Parrinello, M. *J. Chem. Theory Comp.* **2012** *8*, 2247.

33) De Meyer, T. ; Ensing, V; Rogge, S. M. J.; De Clerck, K.; Meijer, E.J.; Van Speybroeck, V. *ChemPhysChem* **2016**, *17*, 3447.

34) Allen M. P. ; Tildesley, D.J. *Computer Simulation of Liquids*, Clarendon, Oxford, 1987.

35) Georg, H. C ; Coutinho, K.; Canuto, S. *J. Chem. Phys*. **2007**, *126*, 034507.

36) Coutinho, K. ; Canuto, S. *J. Chem. Phys*. **2000**, *113*, 9132.

37) Oliveira, L.B.A. ; Prado, R. C.; Júnior, L.A. ; Colherinhas, G. *J. Mol. Liq.* **2018**, *263*, 334.

38) Adamo, C.; Barone, V. *J. Chem. Phys*. **1999**, *110*, 6158.

39) Ditchfield, R. ; Hehre, W. J.; Pople, J. A. *J. Chem. Phys.* **1971**, *54*, 724.

40) Grimme, S. ; Antony, J. ; Ehrlich, S.; Krieg, H. *J. Chem. Phys*. **2010**, *132*, 154104.

41) Chai, J.-D. ; Head-Gordon, M. *Phys. Chem. Chem. Phys*. **2008**, *10*, 6615.

42) Jacquemin, D.; Perpète, E. A.; Scuseria, G. E. ; Ciofini, I. ; Adamo, C. *J. Chem. Theory Comp.* **2008**, *4*, 123

43) Scalmani, G.; Frisch, M. J. *J. Chem. Phys.* **2010**, *132*,114110

44) Wang, J.; Wolf, R. M.; Caldwell, J. W.; Kollman, P.A.; Case, D. A. **2004**, *25*, 1157.

45) Gaussian 16, Revision C.01, Frisch, M. J.; Trucks, G. W.; Schlegel, H. B.; Scuseria, G. E.; Robb, M. A.; Cheeseman, J. R.; Scalmani, G.; Barone, V.; Petersson, G. A.; Nakatsuji, H.; Li, X.; Caricato, M.; Marenich, A. V.; Bloino, J.; Janesko, B. G.; Gomperts, R.; Mennucci, B.; Hratchian, H. P.; Ortiz, J. V.; Izmaylov, A. F.; Sonnenberg, J. L.; Williams-Young, D.; Ding, F.; Lipparini, F.; Egidi, F.; Goings, J.; Peng, B.; Petrone, A.; Henderson, T.; Ranasinghe, D.;

Zakrzewski, V. G.; Gao, J.; Rega, N.; Zheng, G.; Liang, W.; Hada, M.; Ehara, M.; Toyota, K.; Fukuda, R.; Hasegawa, J.; Ishida, M.; Nakajima, T.; Honda, Y.; Kitao, O.; Nakai, H.; Vreven, T.; Throssell, K.; Montgomery, J. A., Jr.; Peralta, J. E.; Ogliaro, F.; Bearpark, M. J.; Heyd, J. J.; Brothers, E. N.; Kudin, K. N.; Staroverov, V. N.; Keith, T. A.; Kobayashi, R.; Normand, J.; Raghavachari, K.; Rendell, A. P.; Burant, J. C.; Iyengar, S. S.; Tomasi, J.; Cossi, M.; Millam, J. M.; Klene, M.; Adamo, C.; Cammi, R.; Ochterski, J. W.; Martin, R. L.; Morokuma, K.; Farkas, O.; Foresman, J. B.; Fox, D. J. Gaussian, Inc., Wallingford CT, 2016.

46) Plimpton, S. *J Comp Phys*, **1995**, *117*, 1

47) Würthner, F.; Yao, S.; Debaerdemaeker, T.; Wortmann, R. *J. Am. Chem. Soc*. **2002**, *124*, 9431.

48) Jacquemin, D.; Adamo, C. *J. Chem. Theory Comput.* **2011**, *7*, 369.

49) Wykes, M.; Su, N. Q.; Xu, X.; Adamo, C. ; Sancho-García, J.-C. *J. Chem. Theory Comput.* **2015**, *11*, 832.

50) Jacquemin, D.; Zhao, Y.; Valero, R.; Adamo, C.; Ciofini, I.; Truhlar, D. G. *J. Chem. Theory Comput.* **2012**, *8*, 1255.

Table 1. Computed λ_{max} (in eV) considering the dioxane as solvent and using a static and a MC approach All the electronic transitions were computed at the PBE0/IEF-PCM level of theory, except for the values in parenthesis, which were evaluated using the ωB97XD/IEF-PCM model. Mean Absolute Deviation (MAD in eV) with respect to the experimental values is also reported.

	Monomer					**Dimer**		
	static	MC	static/dimer[a]	MC/dimer[b]	exp[c]	Static	MC	exp[c]
1	2.60 (2.65)	2.46 (2.49)	2.55	2.45	2.18	2.84 (2.96)	2.66 (2.72)	2.52
2	2.38	2.19	2.34	2.18	1.96	2.54	2.37	2.22
3a	3.16	2.89	3.12	2.89	2.68	3.30	3.04	2.89
3b	2.69	2.49	2.65	2.42	2.19	2.87	2.64	2.42
4	2.87	2.70	2.84	2.68	2.41	2.99	2.81	2.60
MAD[d]	0.46	0.26	0.42	0.24		0.38	0.17	

a) computed as the average value of the two monomers at their static geometry in the dimer; b) computed as the average value of the two monomers at their MC geometry in the dimer; c) from reference 47; d) Mean Absolute Deviation

Table 2. Computed main geometrical parameters corresponding to the static approach or averaged MC simulations. The energy differences (ΔE) between optimized PBE0 and MC structures are also reported. Values in parenthesis refer to structures optimized with the ωB97XD functionals.

	Monomer					Dimer						
	θ[a] (degrees)		BLA[b] (Å)		ΔE (kcal/mol)	θ (degrees)		BLA (Å)		center of mass[c] (Å)		ΔE (kcal/mol)
	static	MC	static	MC		static	MC	static	MC	static	MC	
1	3.0 (1.0)	1.8	0.023 (0.024)	0.007	-3.8	13.1 (12.7)	4.4	0.042 (0.06)	0.024	5.137 (5.080)	5.450	-7.1
2	8.0	3.8	0.017	0.023	-3.2	44.1	2.6	0.038	0.018	5.610	4.320	-14.2
3a	0.4	4.0	0.008	0.003	-3.3	48.9	2.1	0.011	0.030	4.110	4.360	-6.1
3b	5.3	7.6	0.015	0.038	-3.2	55.8	8.4	0.007	0.026	3.908	4.350	-6.7
4	1.6	1.8	0.012	0.024	-4.3	8.9	3.0	0.033	0.011	4.770	5.632	-9.0

a) refer to Figure 4b. b) Refer to Figure 4a , c) refer to text for further explanation.

Figure captions

Figure 1. Sketch of merocyanine dyes considered in the present paper. Bu=butyl, Hex=hexyl

Figure 2. Schematic illustration of the stochastic approach.

Figure 3. Illustration of the HOMO/LUMO computed for merocyanines monomers. Blue/ yellow regions indicate the negative/positive isosurfaces.

Figure 4. Optimized static (left) and Monte Carlo averaged structures (right) for molecule **1** (a and b) and **4** (c and d)

Figure 5. Optimized static (left) and Monte Carlo averaged structures (right) for dimers ofmolecules **1** (a and b), **2** (c and d) and **3b** (e and f)

Figure 6. Absorption spectra of dimer **1** in 1,4 dioxane computed with the static (blue dashed line) and stochastic (green solid line) approaches. The experimental spectrum is also reported for comparison (red line)

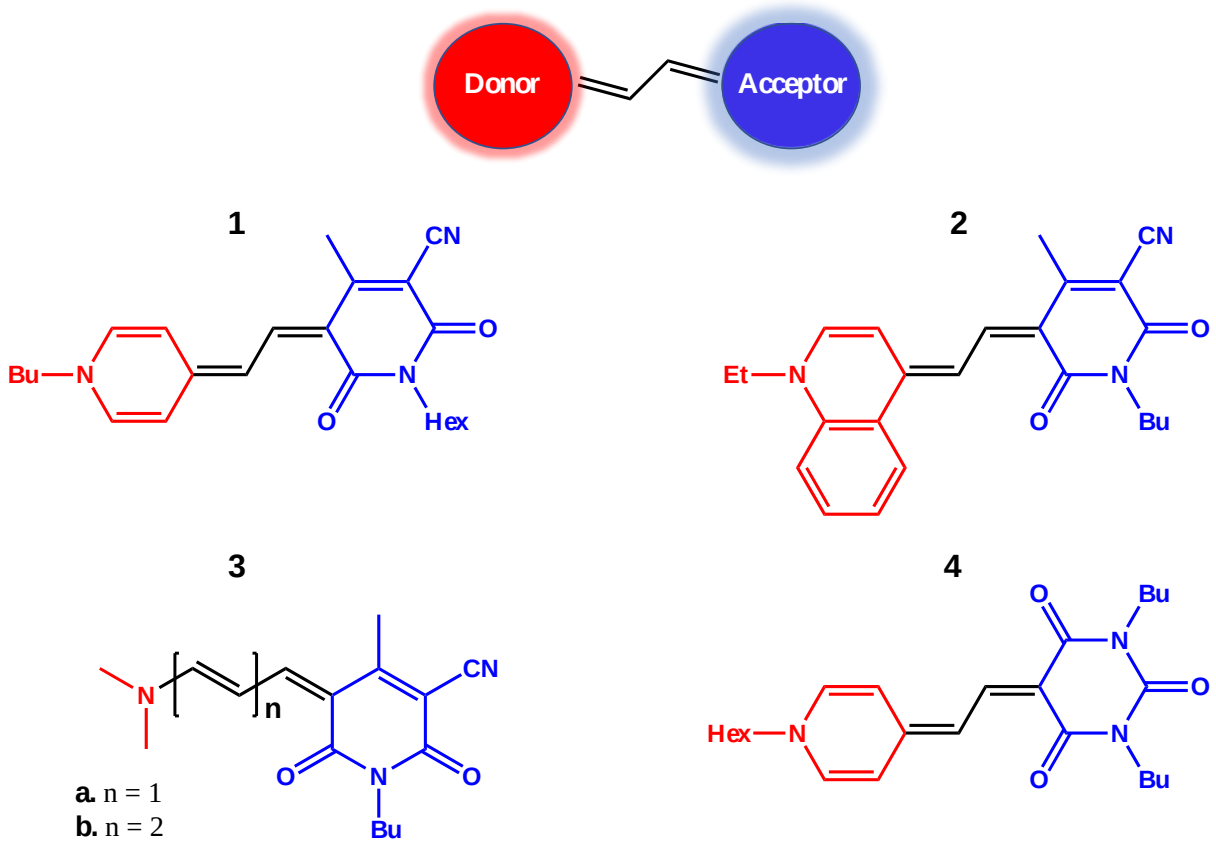
Donor
Acceptor
1
CN
Bu
N
O
N
O
Hex
2
CN
Et
N
O
N
O
Bu
3
CN
N
n
O
N
O
Bu
a. n = 1
b. n = 2
4
O
Bu
N
O
Hex
N
N
O
O
Bu

Figure 1

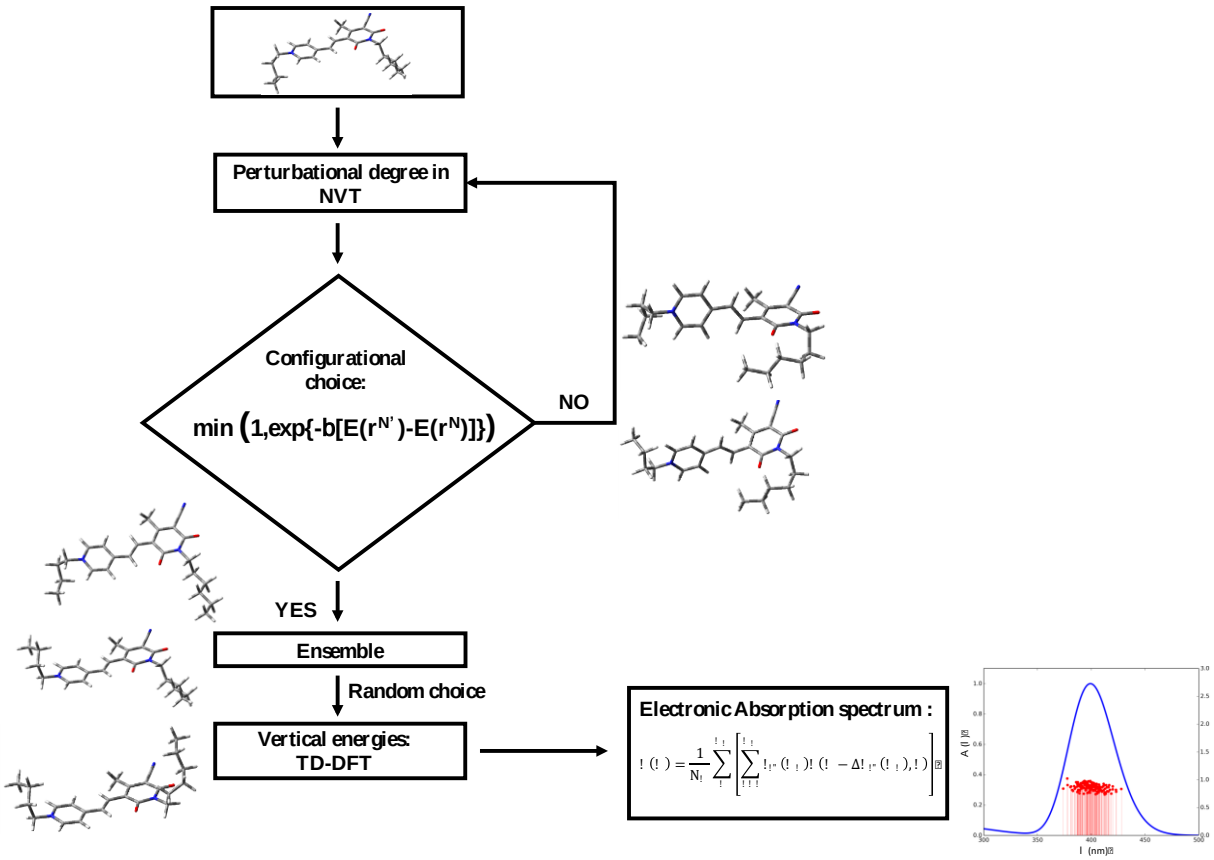
Perturbational degree in NVT
Configurational choice:
min (1,exp{-b[E(r^N')-E(r^N)]})
NO
YES
Ensemble
Random choice
Vertical energies: TD-DFT
Electronic Absorption spectrum :

Figure 2

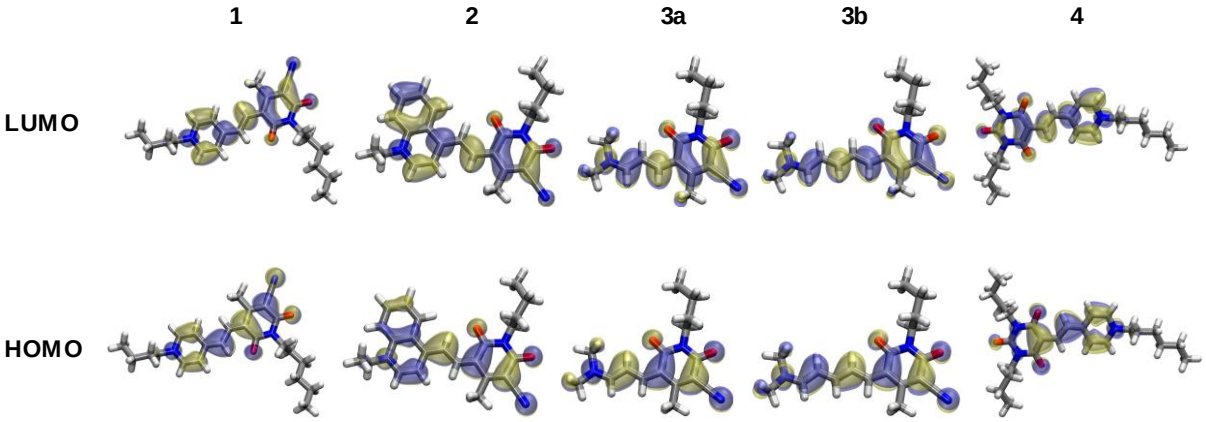

Figure 3

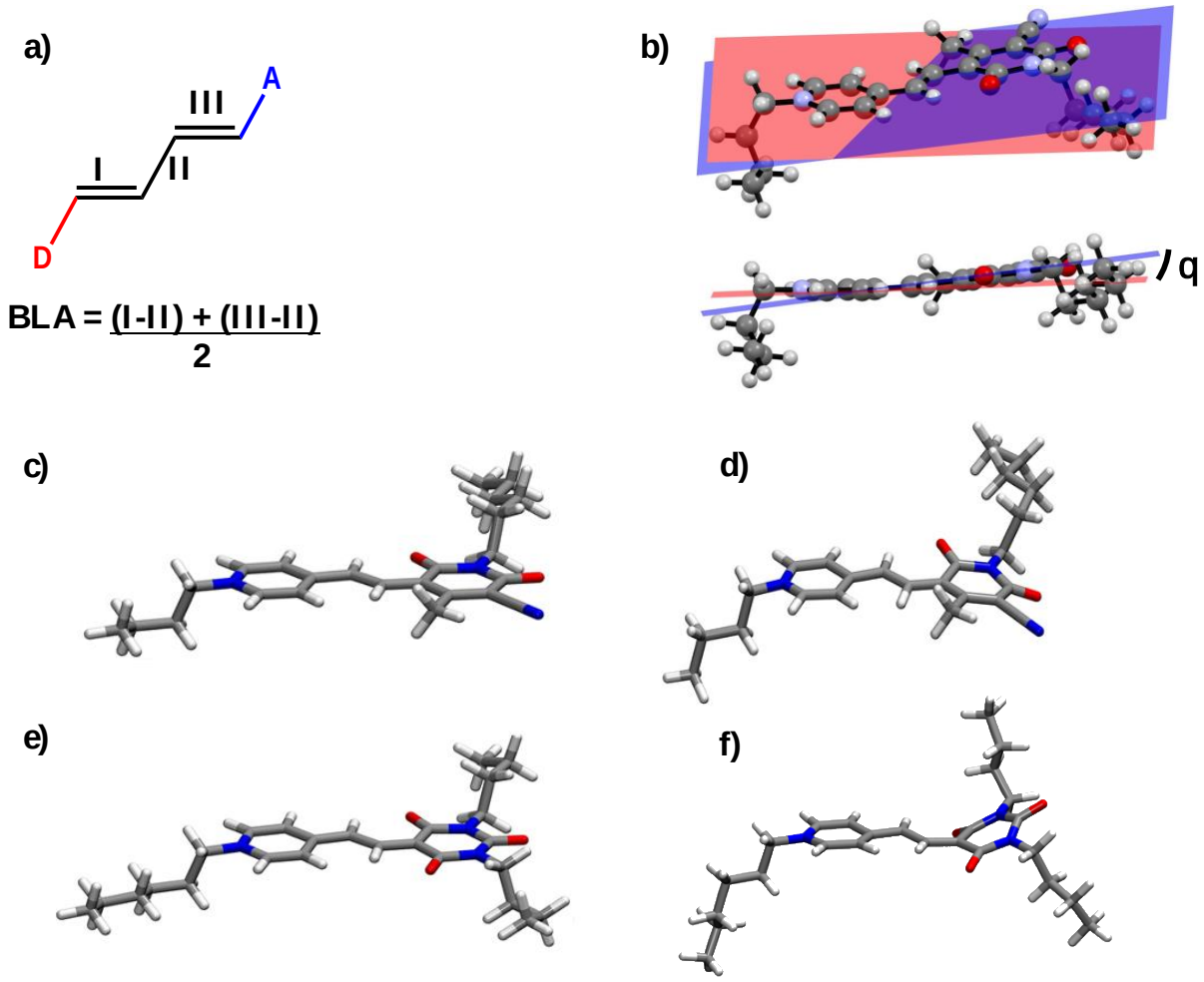

Figure 4

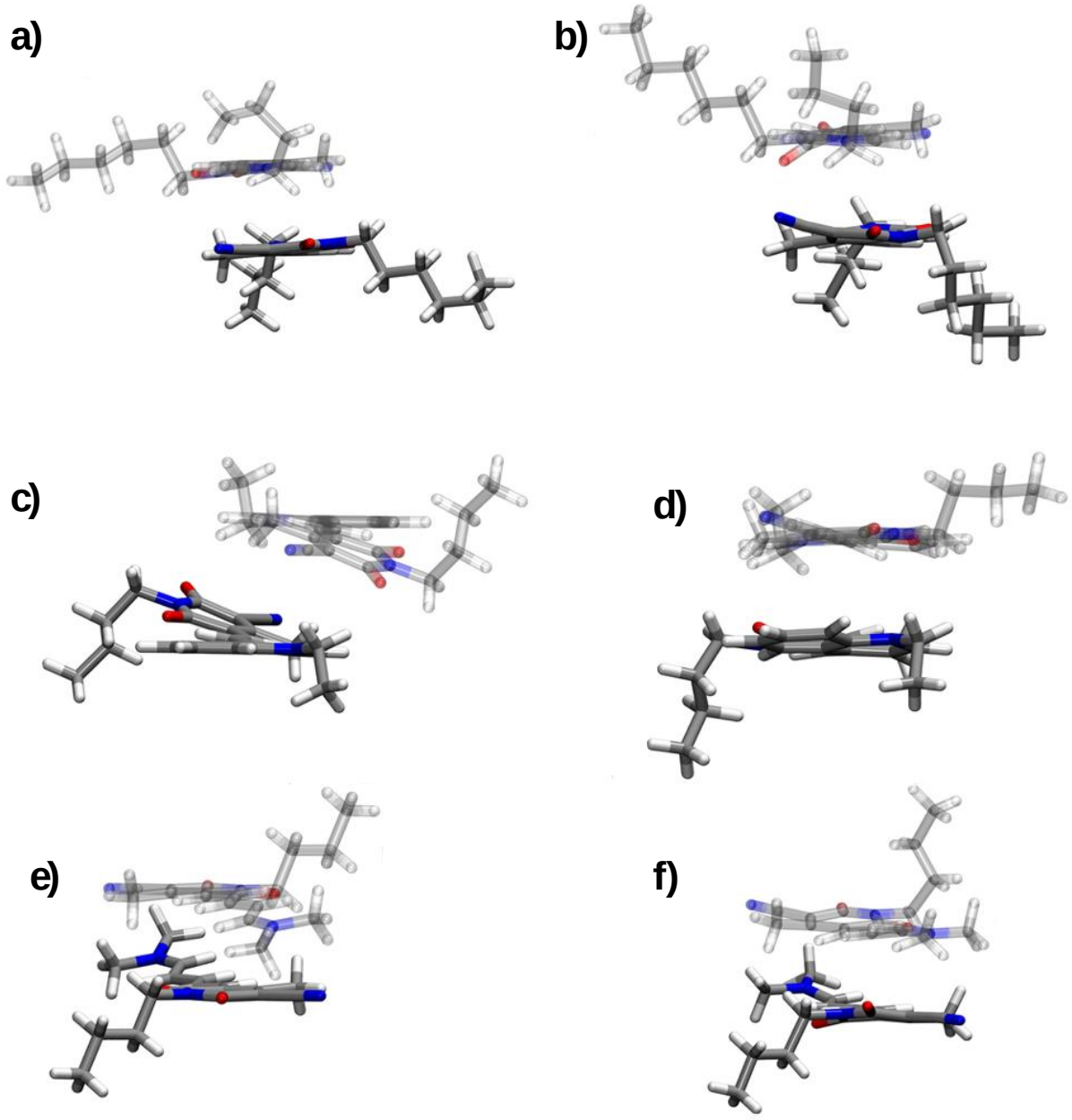

Figure 5

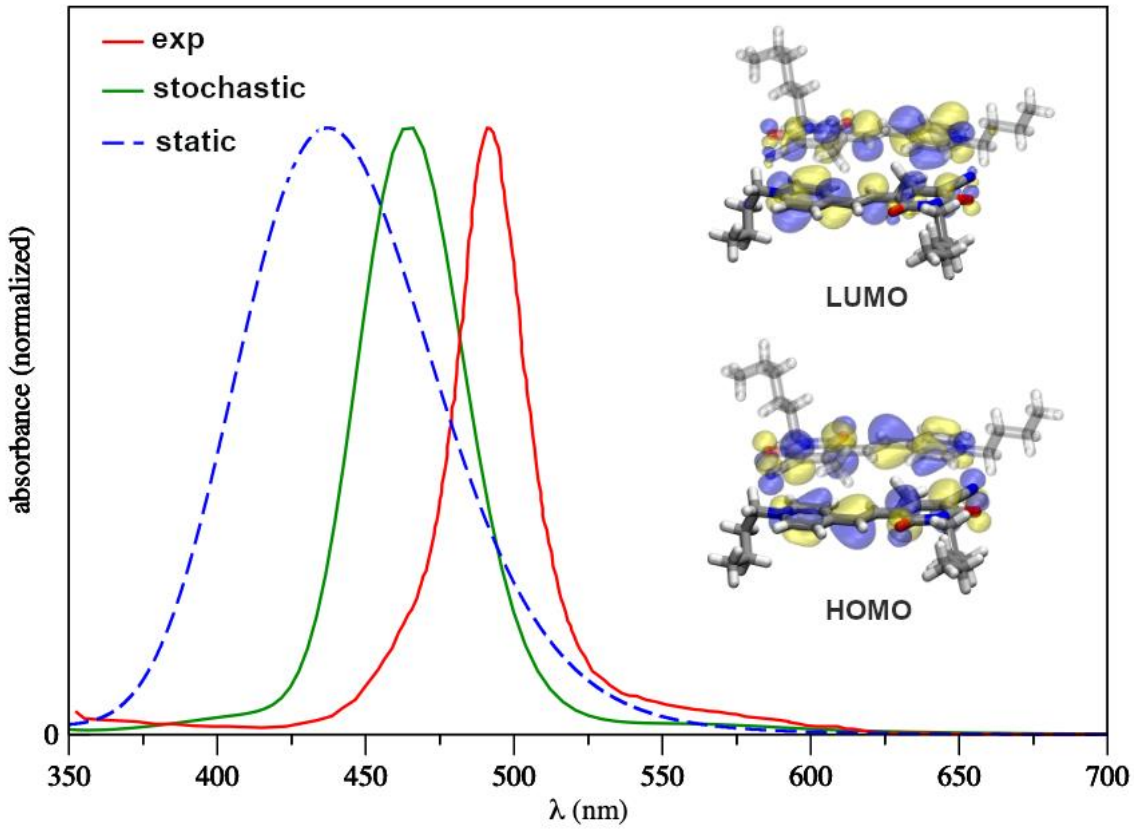
exp
stochastic
static
absorbance (normalized)
0
350
400
450
500
550
600
650
700
λ (nm)
LUMO
HOMO

Figure 6.